Copper-67 Radioimmunotherapy and Growth Inhibition by Anti–L1-Cell Adhesion Molecule Monoclonal Antibodies in a Therapy Model of Ovarian Cancer Metastasis

Karin Knogler,[1] Jürgen Grünberg,[1] Kurt Zimmermann,[1] Susan Cohrs,[1] Michael Honer,[2] Simon Ametamey,[2] Peter Altevogt,[3] Mina Fogel,[4] P. August Schubiger,[1,2] and Ilse Novak-Hofer[1]

Abstract

Purpose: We examined the tumor-targeting and therapeutic effects of ^{67}Cu-labeled single amino acid mutant forms of anti-L1 monoclonal antibody chCE7 in nude mice with orthotopically implanted SKOV3ip human ovarian carcinoma cells.

Experimental Design: For radioimmunotherapy, chCE7 antibodies with a mutation of histidine 310 to alanine (chCE7H310A) and a mutation of asparagine 297 to glutamine (chCE7agl) were generated to achieve more rapid blood clearance. Biodistributions of ^{67}Cu-4-(1,4,8,11-tetraazacyclotetradec-1-yl)-methyl benzoic acid tetrachloride (CPTA)–labeled mutant antibodies were measured in nude mice bearing SKOV3ip human ovarian cancer metastases. The effects of single i.v. injections of ^{67}Cu-chCE7agl alone on tumor reduction and survival were investigated. In addition, a combination of low-dose ^{67}Cu-radioimmunotherapy with unlabeled anti-L1 antibody L1-11A on survival was investigated.

Results: ^{67}Cu-CPTA-chCE7agl showed high (up to 49% ID/g) and persistent (up to 168 h) uptake in SKOV3ip metastases, with low levels in normal tissues. ^{67}Cu-CPTA-chCE7H310A revealed a shorter half-life in the blood and a lower tumor uptake and retention. A single low dose of 4 MBq of ^{67}Cu-chCE7agl reduced tumor growth but did not prolong survival significantly, whereas a single 10.5 MBq dose of ^{67}Cu-chCE7agl reduced tumor growth and prolonged survival significantly. The combination of unlabeled monoclonal antibody L1-11A with a subtherapeutic dose of ^{67}Cu-radioimmunotherapy also prolonged survival significantly.

Conclusion: The results show improved pharmacokinetics and biodistributions as well as the therapeutic effect of the ^{67}Cu-labeled single amino acid mutant chCE7agl. Therapeutic data indicate, for the first time, the feasibility of combining anti–L1-directed growth inhibition and ^{67}Cu-radioimmunotherapy, thereby increasing the efficiency of antibody treatment of metastatic ovarian carcinoma.

Ovarian cancer is often detected late and late-stage disease is characterized by widespread peritoneal dissemination and ascites. Although therapies have been further developed in the past decade, all established therapies reveal a poor effectiveness in the late stage of the disease. Despite improved 5-year survival rates, recurrences are frequent, overall mortality remains unchanged, and new therapeutic strategies are urgently needed. Monoclonal antibodies (mAb) acting by stimulating the immune response such as anti–CA-125 oregovomab (1) and anti–vascular endothelial growth factor antibody bevacizumab, which inhibits angiogenesis, are in phase III trials as adjuvant therapies (1–3). At present, the use of radioimmunotherapy in the treatment of advanced ovarian cancer following cytoreductive surgery and chemotherapy is limited. In a large phase III study, i.p. administration of ^{90}Y-labeled anti-MUC1 antibody, HMFG1, was not found to improve long-term survival (4). Also, radioimmunotherapy using ^{131}I-labeled mAb, OC-125, showed little therapeutic benefit in patients with ovarian cancer (5). Antibodies used in radioactive form for the imaging and radioimmunotherapy of ovarian cancer were directed against MUC1 and CA-125 proteins. Both proteins have large, multivalent, and highly glycosylated mucin-type exodomains. They are shed in high amounts from tumor cells and therefore antibody targeting may be impaired. In addition, the anti-MUC1 and anti–CA-125 antibodies that were used are not actively internalized into target tumor cells, which may also limit their efficacy as targeting vehicles.

Authors' Affiliations: [1]Center for Radiopharmaceutical Science, ETH-PSI-USZ, Paul Scherrer Institute, Villigen, Switzerland; [2]Federal Institute of Technology, Zürich, Switzerland; [3]German Cancer Research Center, Heidelberg, Germany; and [4]Department of Pathology, Kaplan Medical Center, Rehovot, Israel

Received 6/22/06; revised 10/5/06; accepted 10/26/06.

Grant support: Swiss National Science Foundation grant 3100A0-100200 (I. Novak-Hofer) and Schwerpunktprogramm "Invasion und Metastasisierung" Deutsche Krebshilfe (P. Altevogt).

The costs of publication of this article were defrayed in part by the payment of page charges. This article must therefore be hereby marked *advertisement* in accordance with 18 U.S.C. Section 1734 solely to indicate this fact.

Note: K. Knogler and J. Grünberg contributed equally to this study.

Requests for reprints: Ilse Novak-Hofer, Center for Radiopharmaceutical Science, ETH-PSI-USZ, Paul Scherrer Institute, CH-5232 Villigen, Switzerland. Phone: 41-56-310-4067; Fax: 41-56-310-2849; E-mail: ilse.novak@psi.ch.

doi:10.1158/1078-0432.CCR-06-1486

Recently, antibody therapy directed against the L1-cell adhesion molecule protein has emerged as a new option for targeting ovarian cancer metastases (6). L1 is a cell surface protein, originally studied intensively in the nervous system (7–9), which is overexpressed in a number of different tumors, such as neuroblastomas (10), renal carcinomas (10, 11), ovarian, endometrial carcinomas, and melanomas (12). A soluble form of L1 was found in the serum of patients with ovarian cancer and may turn out to be a marker for progression of this disease (13). L1 is increasingly recognized as a signaling molecule which directly and indirectly transmits signals regulating proliferation, migration, and invasion of tumor cells (14–16). Anti-L1 antibodies were found to inhibit tumor cell proliferation *in vitro* (6, 17), and recently, it was shown that the anti-L1 antibody L1-11A inhibits the growth of SKOV3ip human ovarian cancer metastases *in vivo* in nude mice (6). Based on these results, we investigated in this study if the efficacy of antibody treatment was increased by combining the growth inhibition activity of anti–L1-antibodies with radioimmunotherapy using radiometal-labeled anti-L1 antibodies directed against another epitope.

For radioimmunotherapy, the metallic radionuclide ^{67}Cu was selected. Its appropriate half-life of 2.6 days and high abundance of medium energy β-emission of 141 keV make it a suitable option to the high-energy β-emitter ^{90}Y for the treatment of small tumor masses. The lower percentage of therapeutically useless gamma-emission (16% of 93 keV and 48% of 185 keV) compares favorably with the commonly used ^{131}I (82% of 364 keV). Anti-L1 mAb chCE7 binds to target tumor cells with picomolar affinity ($K_d \sim 10^{10}$ mol/L) and inhibits cell proliferation (6, 18). ChCE7 is internalized into target cells, shows high uptake in tumor xenografts in nude mice when used in radioiodinated or in radiocopper-labeled form (19, 20), and performs well in imaging of metastases in patients with neuroblastoma (21). For radioimmunotherapeutic applications, it was of interest to develop variant antibodies with more rapid clearance from the blood because dose-limiting toxicity is usually directed against the blood cells and the bone marrow. To circumvent the low tumor uptake and accumulation of radioactivity in the kidneys observed with rapidly clearing radiometal-labeled antibody fragments, chCE7 antibodies with single amino acid mutations were constructed with no overall change in molecular weight (150 kDa). An aglycosylated form of mAb chCE7 (chCE7N297Q), as well as a single amino acid mutant which had been shown to decrease the half-life of IgG_1 by interfering with FcRn receptor binding (chCE7H310A), were produced (22, 23). Both single amino acid mutants cleared more rapidly from the blood than the parent mAb chCE7. Based on clearance properties and biodistribution data, we selected ^{67}Cu-chCE7agl as radioimmunoconjugates for the therapy of nude mice with SKOV3ip human ovarian cancer metastases. We found that radioimmunotherapy using a single 10.5 MBq dose of the ^{67}Cu-immunoconjugate prolonged survival for a significantly longer time than biweekly treatment with unlabeled mAb L1-11A alone. A single low 5 MBq dose of the ^{67}Cu-immunoconjugate led to significantly increased survival when combined with biweekly treatment with unlabeled mAb L1-11A. Our study shows proof of principle of combining radioactive and inactive anti–L1-cell adhesion molecule mAbs for more efficient therapy of ovarian cancer.

Materials and Methods

Materials. Chemicals and solvents used were from Fluka (Buchs, SG, Switzerland) unless stated otherwise.

Cells and antibodies. HEK-293 cells were from the German Collection of Microorganisms (Braunschweig, Germany), SKOV3ip human ovarian carcinoma cells were previously described (6). HEK-293 and SKOV3ip cells were maintained in DMEM (4.5 g/L glucose). All media were supplemented with 10% FCS, 2 mmol/L of glutamine, 100 units/mL of penicillin, 100 μg/mL of streptomycin, and 0.25 μg/mL of fungizone ("complete medium"). All media and additives were obtained from BioConcept (Allschwil, Switzerland). MAb L1-11A (subclone of UJ127.11) was purified by InVivo Biotech services GmbH (Henningsdorf, Germany).

Antibody design, plasmids, and gene assembly. MAb chCE7 is composed of murine VL and murine VH fused to the Fc part of human $IgG\gamma_1$. The cDNAs for chCE7 light and heavy chain (a gift from J. Jean-Mairet, ETHZ, Switzerland) were cloned into the *Hin*dIII/*Bam*HI site of the mammalian expression vector pcDNA3.1+ (Invitrogen, Basel, Switzerland). Specific mutations were introduced in the CH2 domain of chCE7 heavy chain using overlapping PCR and standard molecular biology techniques (24). For the first PCRs, the following primer pairs were used (*a*) MCSF (5′-GCTGGCTAGCGTTTAAACTTAAGC-3′) and CE7aglR (5′-CACCCGGTACGTGCTTTGGTACTGCTCCTCCC-3′); (*b*) CE7aglF (5′-GGGAGGAGCAGTACCAAAGCACGTACCGGGTG-3′) and CH3R (5′-GCGGATCCTCATTTACCCGGAGACAGGGAGAG-3′); (*c*) MCSF (5′-GCTGGCTAGCGTTTAAACTTAAGC-3′) and CE7H310AR (5′-CCATTCAGCCAGTCCTGGGCCAGGACGGTGAGGACGC-3′); (*d*) CE7H310AF (5′-GCGTCCTCACCGTCCTGGCCCAGGACTGGCTGAATGG-3′) and CH36HISR (5′-GCGGATCCTCAATGGTGATGGTGATGATGTTTACCCGGAGACAGGGAGAG-3′); (*e*) MCSF (5′-GCTGGCTAGCGTTTAAACTTAAGC-3′) and dCH2R (5′-CCTGTGGTTCTCGGGGCTGCCCTGGGCACGGTGGGCATGTGTG-3′); (*f*) dCH2F (5′-CACACATGCCCACCGTGCCCAGGGCAGCCCCGAGAACCACAGG-3′) and CH36HISR (5′-GCGGATCCTCAATGGTGATGGTGATGATGTTTACCCGGAGACAGGGAGAG-3′). After gel purification, the primary PCR products were mixed (1 + 2; 3 + 4; 5 + 6) and a second PCR using the outside primers (MCSF and CHBR for 1 + 2; MCSF and CH36HISR for 3 + 4 and for 5 + 6) was done. The chCE7H310A mutant, the chCE7δCH2 mutant, and the chCE7F(ab′)$_2$ fragment have a 6× His tag at the COOH-terminal end of the heavy chain for affinity purification via Ni-NTA agarose (Qiagen, Basel, Switzerland). All mutations were confirmed by DNA sequencing (Microsynth, Balgach, Switzerland).

Expression, selection, and purification of single amino acid mutants of mAb chCE7. HEK-293 human embryonic kidney cells (1×10^6) were cotransfected with pcDNA3chCE7L (light chain mutant) and pcDNA3chCE7H (heavy chain mutant), and clones were selected with G418 (25). Antibody production was verified with a Slot-Blot method (25). Mutant mAbs were purified from tissue culture supernatants either with protein G-Sepharose (chCE7 and chCE7agl; Amersham Biosciences, Dübendorf, Switzerland) or with Ni-NTA-Sepharose [chCE7H310A, chCE7ΔCH2, and chCE7F(ab′)$_2$] followed by size exclusion chromatography using a Superdex 200 HR 10/30 column (Amersham Biosciences).

Characterization of purified chCE7 single amino acid mutants. Purified proteins were analyzed by SDS-PAGE under reducing and nonreducing conditions and by size exclusion chromatography on a Superdex 200 column at 0.5 mL/min flow rate using PBS buffer [0.1 mol/L NaCl and 0.05 mol/L sodium phosphate buffer (pH 7.4)].

The affinities of mutant antibodies were measured by binding assays with SKOV3ip cells. Competition binding assays were done by incubating triplicate samples of a fixed concentration of ^{125}I-labeled chCE7 (50 ng) and increasing concentrations of unlabeled competitors (chCE7, chCE7agl, chCE7H310A; 1-3,000 ng) with 0.5×10^6 SKOV3ip cells suspended in 500 μL of PBS containing 0.5% bovine serum albumin

on a shaking platform for 2 h at 37°C. Nonspecific binding was determined by parallel incubations in the presence of 10 μg of unlabeled competitor. After incubation, cells were washed twice with PBS containing 0.5% bovine serum albumin to remove unbound immunoconjugates and cell-bound radioactivity was measured with a gamma counter (CobraII Packard, Canberra Packard GmbH, Frankfurt, Germany). Binding of ^{67}Cu-labeled antibodies to SKOV3ip cells was measured by incubating cells with radiocopper-labeled tracers in a concentration range between 800 and 25 ng. Nonspecific binding in the presence of 10 μg of unlabeled mAb chCE7 was subtracted and data was analyzed with the GraphPad prism program using the Scatchard method.

Internalization of radiocopper-labeled immunoconjugates into SKOV3ip cells was measured as described earlier (19). Briefly, triplicate samples of adherent 2×10^6 SKOV3ip cells were incubated with 3 kBq (150 ng) of ^{67}Cu-labeled antibodies in complete DMEM medium for 4 h on ice. Unbound antibodies were washed off with PBS, fresh medium was added, and cells were incubated at 37°C for 2, 16, and 24 h. One set of cells (time 0) was processed directly by measuring acid-0released radioactivity using 0.1 mol/L of NaCl and 0.05 mol/L of glycine (pH 2.8). Cells were dissolved in 1 mol/L of NaOH and acid stable, cell-bound radioactivity was measured. Internalized radioactivity was defined as the percentage of acid stable activity of total cell-bound activity.

Ligand substitution of chCE7 antibodies. For labeling with ^{67}Cu, the proteins were substituted with 4-(1,4,8,11-tetraazacyclotetradec-1-yl)-methyl benzoic acid tetrachloride (CPTA), which was synthesized and attached as a succinimide ester to chCE7 antibodies as previously described (26). Using an isotope dilution assay, it was estimated that there were four CPTA ligands for each mAb (26).

Radiolabeling. Radioiodination of chCE7 antibodies (100 μg) in PBS was done with the Iodogen method (Pierce, Perbio Science, Lausanne, Switzerland) as described previously (18).

^{67}Cu was produced in-house by irradiating natZn with protons at the 72 MeV accelerator of the Paul Scherrer Institute (Villigen, Switzerland) as described before (27), and used for radiolabeling 1 day after production. For the positron emission tomography (PET) imaging experiments, ^{64}Cu was produced at the Paul Scherrer Institute as described before (26).

Two hundred to 400 μg (250 μL) of the immunoconjugates in a total volume of 500 μL of 0.1 mol/L sodium acetate buffer (pH 5.5) 18.5 to 30 MBq (500-800 μCi) of neutralized ^{67}Cu solution. For producing large amounts of radiolabeled conjugates for therapeutic experiments, up to 3 mg of ligand-substituted antibodies were labeled with up to 300 MBq of ^{67}Cu for 30 min at 22°C. After incubations, EDTA was added to a final concentration of 5 mmol/L for 5 min to complex unchelated copper. Purification of the labeled antibodies was achieved by fast protein liquid chromatography size exclusion chromatography on a Superdex 200 column (Amersham Biosciences) in PBS at a flow rate of 1.0 mL/min.

Quality control of radiolabeled preparations. Radiolabeled immunoconjugates were analyzed by size exclusion chromatography on a Superose 12 column (Amersham Biosciences) at 0.5 mL/min flow rate using PBS buffer. The major peaks of mAb eluted with a retention time of 22.50 min for ^{67}Cu-chCE7, 22.50 min for ^{67}Cu-chCE7agl, and 23.60 min for ^{67}Cu-chCE7H310A. The EDTA-metal complex appeared with a retention time of 34 to 35 min. The immunoreactivity of the ^{67}Cu-chCE7 preparations were assayed with a cell-binding test using increasing numbers of SKOV3ip cells as described before (28). The stability of the labeled antibodies (6 μg, 160 MBq) was analyzed after incubation in human plasma of radioimmunoconjugates in 2.0 mL of human plasma at 37°C. After the addition of 5 mmol/L of EDTA, samples (0.5 mL) were separated by fast protein liquid chromatography on a Superdex 200 HR 10/30 column (Amersham Biosciences) in PBS as described (29). Fractions (0.5 mL) were collected and radioactivity was measured in a gamma counter.

Pharmacokinetic and biodistribution studies. All animal studies were conducted in compliance with Swiss laws on animal protection. Housing and animal husbandry was done according to local laws on animal protection. For measuring the clearance of antibodies from the blood, groups of five female 6-week-old BALB/c mice were injected with ~370 kBq (10 μCi) of radiolabeled conjugates into the tail vein. Protein content was 7 μg in the case of ^{67}Cu-chCE7, 30 μg in the case of ^{67}Cu-chCE7agl, and 80 μg in the case of ^{67}Cu-chCE7H310A. At timed intervals after injection, blood samples (2 μL) were collected from the tail vein and measured together with an aliquot of the injected solution in a gamma counter. ^{125}I emission was read at a window of 15 to 70 keV, whereas for ^{67}Cu, an energy window between 160 and 210 keV was used. Results are expressed as the percentage of injected dose per total amount of blood (% ID/2 mL). Pharmacokinetic variables were determined using a two-compartment model and the equation $cp(t) = A_\alpha \times e^{-\alpha t} + A_\beta \times e^{-\beta t}$, where the first part of the equation corresponds to the distribution phase and the second part to the terminal elimination phase. The areas under the curve were calculated using the GraphPad Prism program.

For biodistribution studies, female nude mice, 5 weeks old (CD1-foxn1^{nu}; Charles River, Inc., Sulzfeld, Germany) were injected i.p. with 5×10^6 SKOV3ip human ovarian carcinoma cells. Two weeks later, ^{67}Cu-labeled chCE7 antibody conjugates were injected into the tail vein at the concentrations indicated. At 16, 24, 48, 96, 120, and 168 h postinjection, groups of four animals were sacrificed and dissected. Tumors and major organs were weighed and measured together with an aliquot of the injected solution in a gamma counter. Results are expressed as the percentage of injected dose per gram (% ID/g). Statistical analysis of data was done with Student's t test (two-tailed, unequal variance).

Therapy studies. Female CD1-foxn1^{nu} mice, 5 weeks old, were injected i.p. with 7×10^6 SKOV3ip cells. Two days postinoculation, 4 MBq (200 μg) or 10.5 MBq (330 μg) of ^{67}Cu-labeled chCE7agl was injected in groups of eight to nine mice. Control animals (11) were left untreated. After 21 days, the animals were euthanized and dissected, tumor weight and ascites weight was measured. In the survival experiments, female CD1-foxn1^{nu} mice, 5 weeks old, were injected i.p. with 7×10^6 SKOV3ip cells or 14×10^6 SKOV3ip cells. After 2 days, random groups of eight or nine animals were formed and ^{67}Cu-labeled antibody conjugates were injected i.v. at the doses indicated. MAb L1-11A (in 300 μL of sterile PBS at a dose of 10 mg/kg) was injected i.p. biweekly. Animals were checked twice a week for weight, visible ascites, and behavioral signs of distress. In three "survival" experiments with ^{67}Cu-labeled chCE7agl alone and in combination with mAb L1-11A, animals were kept until ascites was visible or a weight loss of >15% combined with behavioral signs of distress were observed. At this end point, animals were euthanized.

Statistical analysis. Statistical analysis of data was done using Student's t test (two-tailed, unpaired) and by log-rank test in the case of the survival experiment. In the survival experiment, one animal in the control group and one animal in the ^{67}Cu-chCE7agl–treated group were censored (unexplained death).

PET imaging. For the PET experiments, a tumor-free nude mouse was imaged after i.v. injection of 21 MBq (120 μg) of ^{64}Cu-CPTA-chCE7, prepared as described earlier (26). One mouse was imaged after the injection of 21.5 MBq (150 μg) of ^{64}Cu-CPTA-chCE7 22 days postinoculation of SKOV3ip cells, whereas one mouse was injected with 23 MBq (120 μg) of ^{64}Cu-CPTA mAb L1-11A also 22 days postinoculation of SKOV3ip cells. The animals were anesthetized 21 to 23 h after injection and scanned with a quad-HIDAC PET tomograph (Oxford Positron Systems, Oxford, United Kingdom). PET data were acquired in list mode for 60 to 90 min and reconstructed in a single time frame using the OPL-EM algorithm (0.5 mm bin size, 200-240 240 matrix size). Image files were analyzed using the dedicated software PMOD (30), and depicted as maximal intensity projections.

Immunohistochemistry. Immunostaining of paraffin sections from SKOV3ip tumors was done with anti-L1 antibody (L1-14.10) as described before (31).

Results

Pharmacokinetics of mAb chCE7 variants with single amino acid mutations. In order to select a mAb chCE7 antibody with more rapid clearance from the blood than the parental mAb, a number of chCE7 variant forms were constructed. Medium size divalent F(ab′)$_2$ fragments (100 kDa) and antibodies deleted in the CH2 domain (110 kDa) were produced as described before (25). In addition, chCE7 forms with single amino acid mutations were constructed with no overall change in molecular weight (150 kDa). A mutant mAb with Asn^{297} replaced by Gln and thereby deleted in N-linked glycosylation (chCE7agl) as well as a mutant with His^{310} changed to Ala with decreased affinity for the FcRn receptor (chCE7H310A) was produced. The expression of recombinant proteins included treatment of transfected HEK-293 cells with sodium butyrate and yielded high amounts of antibodies (30 mg/L of purified protein). In a set of competition binding assays, the binding of ^{125}I-chCE7 to SKOV3ip cells in the presence of increasing concentrations of different antibodies was measured. IC$_{50}$ values were 82 ng for chCE7agl, 33 ng for chCE7H310A, and in the same series, the IC$_{50}$ of chCE7 was 75 ng (data not shown). These results indicated that binding affinities of the mutant antibodies were comparable to the wild-type chCE7 antibody.

We next tested the pharmacokinetics of mutant radioiodinated chCE7 antibodies. Figure 1A shows that the clearance from the blood of medium-sized mAb fragments chCE7ΔCH2 and chCE7F(ab′)$_2$ showed similar rapid clearance as expected, followed by chCE7H310A and chCE7agl. The single amino acid mutants were cleared with biphasic kinetics and the differences in $t_{1/2}\alpha$ for the mutant proteins were not statistically different. The order of terminal half-lives ($t_{1/2}\beta$) of blood clearance from the slowest to the fastest was as follows: intact chCE7 > chCE7agl > chCE7H310A. The spectrum of $t_{1/2}\beta$ of radioiodinated antibodies ranged from ~6 days (^{125}I-chCE7) to 10 h (^{125}I-chCE7H310A). The difference between radioiodinated chCE7 and the chCE7agl antibody was statistically significant at all time points ($P < 0.01$). The blood clearance and biodistributions of the radiocopper-labeled chCE7agl and chCE7H310A conjugates were compared with mAb chCE7 (Fig. 1B). The ^{67}Cu-labeled F(ab′)$_2$ fragments were excluded because of the known accumulation of radiometal-labeled medium-sized F(ab′)$_2$ fragments in the kidneys (27). The chCE7ΔCH2 fragment was not chosen because of its tendency to aggregate and its inconvenient handling during ligand substitution and labeling. In contrast, the single amino acid mutant forms of chCE7 had little tendency to aggregate. In a parallel study on stability in human plasma, the ^{67}Cu-CPTA-chCE7agl as well as the ^{67}Cu-CPTA-chCE7 conjugates were stable at 37°C for at least 48 h with no evidence of fragmentation or binding to serum proteins (data not shown). Figure 1B shows clearance from the blood of the ^{67}Cu-labeled immunoconjugates. Statistical analysis of the blood clearance curves showed a significant difference ($P < 0.01$) between radiocopper-labeled chCE7 and the chCE7H310A mutant at all time points, the difference between chCE7 and chCE7agl was significant ($P < 0.05$) at the longest time points (72 and 96 h).

Table 1 summarizes the pharmacokinetic variables of different antibody formats in radioiodinated and radiocopper-labeled form. Table 1 shows, in addition to the α-phase (distribution) and β-phase (terminal elimination) half-lives,

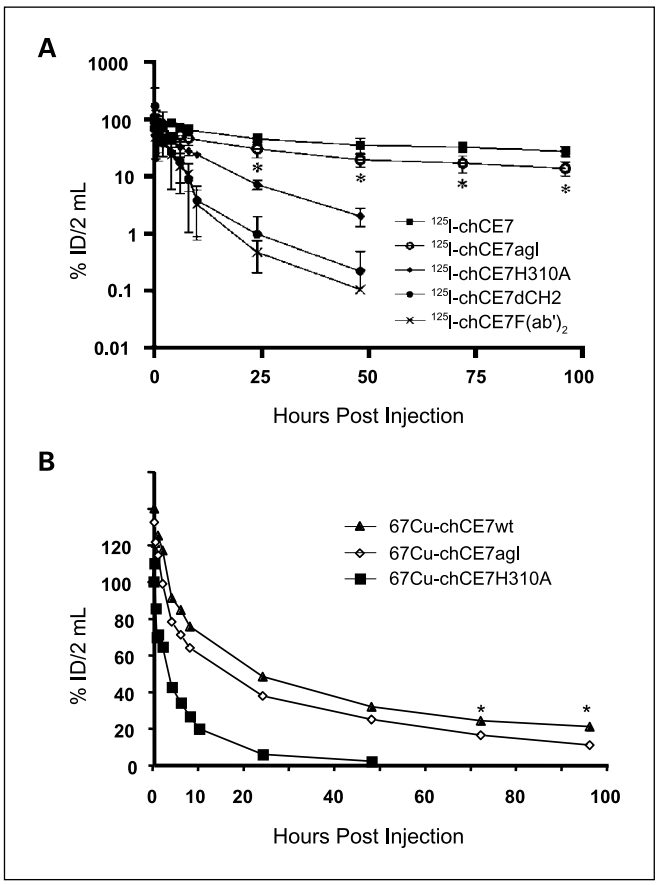

Fig. 1. Clearance from the blood of radiolabeled chCE7 antibody formats. *A,* 370 kBq (7 μg) of ^{125}I-labeled chCE7 mAb formats were injected i.v. At the indicated time points, blood samples were collected from the tail vein and radioactivity was measured. Points, mean percentage of the injected dose of the total amount of blood (% ID/2 mL); bars, SD ($n = 5$). *B,* 370 kBq of ^{67}Cu-labeled chCE7 mAb formats corresponding to 30 μg of ^{67}Cu-chCE7 and ^{67}Cu-chCE7agl, and to 80 μg of ^{67}Cu-chCE7H310A were injected i.v. At the indicated time points, blood samples were collected from the tail vein and radioactivity was measured. Points, mean percentage of the injected dose of the total amount of blood (% ID/2 mL); bars, SD ($n = 5$).

the calculated area under the curve for each construct (% ID/2 mL × h). The mean residence time was calculated as a single variable for blood clearance. Mean residence time as a single variable for blood clearance considers all pharmacokinetic processes which a mAb is exposed to in the body and was found to be 4- to 5-fold lower for the chCE7H310A mutant antibody than for the other antibodies. The difference between the mean residence time of chCE7 and chCE7agl was less pronounced than the difference in terminal half-life $t_{1/2}\beta$.

In vitro *and* in vivo *evaluation of ^{67}Cu-labeled single amino acid mutant of mAb chCE7.* Both ^{67}Cu-labeled chCE7agl and chCE7H310A showed more rapid pharmacokinetics than the parental mAb chCE7 and were potentially suitable for therapy. Tumor uptake and normal tissue distribution in nude mice with SKOV3ip metastases was investigated in order to select the radioimmunoconjugate exhibiting the highest tumor accumulation and the lowest levels in liver and blood for therapy experiments. The nuclide we chose for radioimmunotherapy is the medium-range β-particle emitter, ^{67}Cu ($t_{1/2}$ = 2.6 days). We had previously selected the CPTA chelate as the most stable ligand for copper labeling of intact antibodies (28). Catabolism

Table 1. Pharmacokinetic variables of ^{125}I- and ^{67}Cu-labeled chCE7 single amino acid mutants and wild-type antibody

Antibody formats	$t_{1/2\alpha}$ (h)	A_α (% ID/2 mL)*	$t_{1/2\beta}$ (h)	A_β (% ID/2 mL)	AUC†	MRT (h)‡
^{125}I-chCE7	0.70	55.4	138	45.4	4,015	39.1
^{125}I-chCE7agl	0.59	68.5	96.3	27.8	2,437	35.6
^{125}I-chCE7H310A	2.05	47.4	10.1	46.5	834	8.67
^{67}Cu-chCE7	1.57	64.9	78.9	47.1	3,932	33.1
^{67}Cu-chCE7agl	1.15	52.1	39.3	57.2	3,045	29.5
^{67}Cu-chCE7H310A	0.81	77.6	11.2	31.5	712	9.41

*Y-axis intercept of the two components are given by A_α and A_β, where the sum of A_α and A_β is the total % ID/2 mL.
†The area under the curve (AUC) is a time integral of the blood concentration (% ID/2 mL × h).
‡The mean residence time (MRT) used to give a single variable for blood clearance.

of the internalizing chCE7 antibody exhibited high retention of the Cu-CPTA complex in target tumor cells (19). Approximately four CPTA ligands were substituted per antibody molecule. Immunoreactivity as determined by binding to SKOV3ip cells *in vitro* was 80% to 100% for ^{67}Cu-labeled antibodies. We previously showed that high binding affinity and internalization of chCE7 antibody contribute to the excellent uptake of ^{67}Cu-CPTA-chCE7 in tumor xenografts (18). We therefore investigated binding affinity and internalization of the radiocopper-labeled chCE7agl mutant antibody in SKOV3ip cells.

Figure 2 shows a direct comparison of the two radiocopper immunoconjugates. Binding affinities to SKOV3ip cells were found to be similar ($K_d \sim 6.7 \times 10^{-10}$ mol/L for chCE7wt and 6.9×10^{-10} mol/L for chCE7agl; Fig. 2A). Internalization of the two conjugates was also similar, after 24 h, ~80% of the cell-bound radioactivity was being recovered in the acid stable pool (Fig. 2B). Tumor and tissue uptake of ^{67}Cu-CPTA–labeled mAb chCE7agl was measured in nude mice with SKOV3ip human ovarian cancer metastases.

Table 2 shows biodistributions measured starting 1 day post-i.v. injection up to 5 days for chCE7agl. The immunoconjugate reached a maximal tumor accumulation at 48 h with 49.2 ± 3.95% ID/g. Five days postinjection, the accumulation of radioactivity in normal tissues was low, similar to ^{67}Cu-labeled chCE7 antibody. In the next step, ^{67}Cu-chCE7H310A was compared with ^{67}Cu-chCE7agl. Because of the more rapid blood clearance of chCE7H310A, 16 h was chosen as the starting point for measurements. ^{67}Cu-labeled chCE7H310A reached maximal tumor accumulation at 16 h postinjection with 13.1 ± 2.39% ID/g. Liver uptake for this conjugate was high with 26.1 ± 3.68% ID/g and accumulation in the spleen was 9.2 ± 1.73% ID/g. Radioactivity cleared from the tumor rapidly and reached 2.17 ± 0.65% ID/g 120 h postinjection. When ^{67}Cu-chCE7H310A was compared with ^{67}Cu-chCE7agl at the 24-h time point, the latter showed higher and more persistent tumor uptake (39.7 ± 6.2 versus 9.67 ± 10.7; $P = 0.035$) and lower radioactivity levels in the liver (4.71 ± 0.74 versus 14.70 ± 3.3, $P = 0.010$) than the chCE7H310A mutant with impaired FcRn receptor binding. Because of the more favorable biodistributions ^{67}Cu-CPTA-chCE7agl was selected for further therapy experiments. The chCE7agl antibody was found to inhibit growth of SKOV3ip cells *in vitro* to a similar extent as mAb chCE7 and mAb L1-11A (data not shown).

Antitumor effects of ^{67}Cu-labeled chCE7agl antibody. The SKOV3ip metastasis model was used to assess antitumor effects. Radiocopper-labeled antibodies were injected i.v. 2 days post-i.p. inoculation of 7×10^6 SKOV3ip cells in groups of seven to nine nude mice. In the first experiment, the effect of radioimmunotherapy with two different doses of ^{67}Cu-chCE7agl on progressive growth of SKOV3ip cells was investigated.

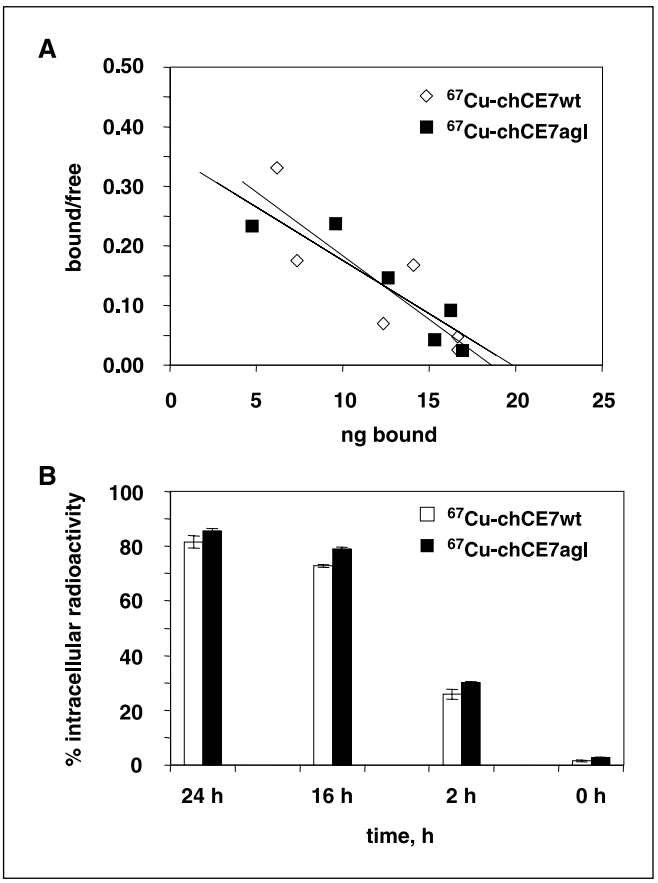

Fig. 2. Binding affinities and internalization of ^{67}Cu-chCE7 and its aglycosylated variant into SKOV3ip cells. *A,* Scatchard plots of saturation binding to SKOV3ip cells, extrapolating to a K_d of 6.7×10^{-10} mol/L for chCE7wt and to 6.9×10^{-10} mol/L for chCE7agl. *B,* intracellular radioactivity (percentage of total cell-bound activity) after internalization of ^{67}Cu-chCE7 and its aglycosylated variant into SKOV3ip cells. Cells were loaded with radiocopper-labeled antibodies at 4°C for 4 h, unbound antibodies were washed off and cells were incubated in complete medium for up to 24 h. Radioactivity in the acid-stable and acid-releasable fraction was measured at the indicated time points. Columns, percentage of acid-stable radioactivity of total cell-bound activity.

Table 2. Biodistributions of ^{67}Cu-labeled chCE7 single amino acid mutants in nude mice with human ovarian cancer (SKOV3ip) metastases

Organ (% ID/g)	24 h	48 h	96 h	168 h	168 h
^{67}Cu-chCE7agl					^{67}Cu-chCE7
Tumor	39.7 (6.23)	49.2 (3.95)	40.2 (4.75)	48.5 (13.4)	34.4 (0.80)
Blood	10.9 (1.70)	8.33 (3.28)	3.27 (2.15)	2.22 (1.17)	1.95 (1.15)
Liver	4.71 (0.74)	4.44 (1.07)	2.80 (0.57)	3.12 (0.87)	5.72 (1.39)
Spleen	3.76 (1.53)	5.37 (1.07)	4.81 (1.18)	4.42 (3.38)	4.74 (2.18)
Kidney	6.02 (0.53)	5.94 (1.38)	4.09 (1.35)	4.36 (0.97)	2.22 (0.63)
Heart	5.53 (1.52)	3.42 (1.09)	1.46 (0.75)	1.72 (0.98)	1.07 (0.32)
Stomach	1.06 (0.31)	1.18 (0.53)	0.89 (0.37)	0.92 (0.38)	0.79 (0.09)
Intestine	1.69 (0.32)	1.42 (0.29)	0.92 (0.30)	0.67 (0.19)	0.91 (0.11)
Muscle	1.34 (0.32)	1.20 (0.61)	0.84 (0.46)	0.41 (0.27)	0.25 (0.20)

Organ (% ID/g)	16 h	24 h	48 h	120 h
^{67}Cu-chCE7H310A				
Tumor	13.1 (2.39)	9.67 (10.7)	6.81 (0.77)	2.17 (0.65)
Blood	1.10 (0.10)	0.34 (0.18)	0.26 (0.08)	0.19 (0.07)
Liver	26.1 (3.68)	14.7 (3.33)	10.7 (5.06)	8.58 (2.47)
Spleen	9.20 (1.73)	4.44 (3.81)	3.39 (1.48)	3.59 (0.25)
Kidney	3.91 (0.49)	2.09 (0.37)	2.16 (0.46)	1.39 (0.22)
Heart	2.88 (0.74)	1.55 (0.34)	1.11 (0.53)	1.83 (0.33)
Stomach	0.92 (0.38)	0.51 (0.24)	0.32 (0.07)	0.53 (0.08)
Intestine	1.78 (0.41)	1.18 (0.54)	0.70 (0.40)	0.59 (0.14)
Muscle	0.07 (0.33)	0.04 (0.19)	0.21 (0.14)	0.12 (0.07)

NOTE: Groups of four animals were injected i.v. with 225 kBq (10 μg) of ^{67}Cu-chCE7agl, 141 kBq (25 μg) of ^{67}Cu-chCE7 and 95 kBq (26 μg) of ^{67}Cu-chCE7 H310A. Data are presented as % ID/g ± SD.

After 21 days, tumor masses and ascites were removed quantitatively.

Table 3 shows that in the control group, 7 of 11 animals developed ascites, whereas in the low-dose radioimmunotherapy group, no ascites had appeared, and in the high-dose radioimmunotherapy, 2 of 9 animals presented with ascites. Both doses led to a significant ~70% decrease in overall tumor burden, the difference between the two dosages was not significant. In the next step, experiments were designed to investigate survival in this late-stage ovarian cancer model by using ^{67}Cu-labeled chCE7agl alone and in combination with unlabeled anti-L1 mAb L1-11A. In a pilot experiment, mice with SKOV3ip metastases were imaged 21 to 23 h postinjection of ^{64}Cu-labeled anti-L1 antibodies.

Figure 3 shows ^{64}Cu-PET imaging of a tumor-free control mouse with mAb chCE7 (A), a mouse with SKOV3ip metastases imaged with anti-L1 mAb chCE7 (B), and a mouse with SKOV3ip metastases imaged with anti-L1 mAb L1-11A (C). The abdominal tumor nodules were visualized well, demonstrating good tumor targeting ability of the two mAbs. Binding experiments to SKOV3ip cells *in vitro* showed that binding of mAb chCE7 was not inhibited by mAb L1-11A and vice versa, indicating that the mAbs bind to different epitopes on L1-cell adhesion molecules (data not shown), and the combination of the two mAbs did not impair their respective tumor-binding abilities. When paraffin sections of SKOV3ip tumors were stained with anti-L1 antibody, L1-14.10, the staining was found to be heterogeneous, with L1-positive tumor cells in the leading edge of the tumor and tumor cells invading and L1-negative cells in the tumor mass (Fig. 3D).

The decrease in tumor mass observed by ^{67}Cu-radioimmunotherapy (Table 3) or by repeated administration of unlabeled mAb L1-11A (6) may not necessarily lead to increased survival. Therefore, survival experiments were done subsequently with groups of seven to nine mice. We defined the end points as the appearance of ascites, which is clearly visible in nude mice, or >15% weight loss, combined with behavioral signs of distress. At this end point, mice were dissected and the tumor mass was

Table 3. L1-directed therapy of orthotopic SKOV3ip tumors in nude mice treated with ^{67}Cu-chCE7agl

Treatment group	Number of mice injected	Mean tumor weight ± SD (g)	P*	Mean ascites (mL)	Mean body weight (g)
Controls	11	1.30 ± 0.69		1.61 (7/11)	23.1 ± 1.8
^{67}Cu-chCE7agl4 MBq	8	0.51 ± 0.23	0.003	0 (0/8)	24.4 ± 1.9
^{67}Cu-chCE7agl10.5 MBq	9	0.38 ± 0.20	0.006	0.30 (2/9)	24.2 ± 1.6

NOTE: SKOV3ip cells (7×10^6 cells) were injected i.p. into nude mice. Treatments consisted of a single i.v. dose of ^{67}Cu-chCE7agl 2 d after postinoculation. On day 21, mice were necropsied and tumor weight, ascites, and body weight were measured.
*Significance level (Student's *t* test).

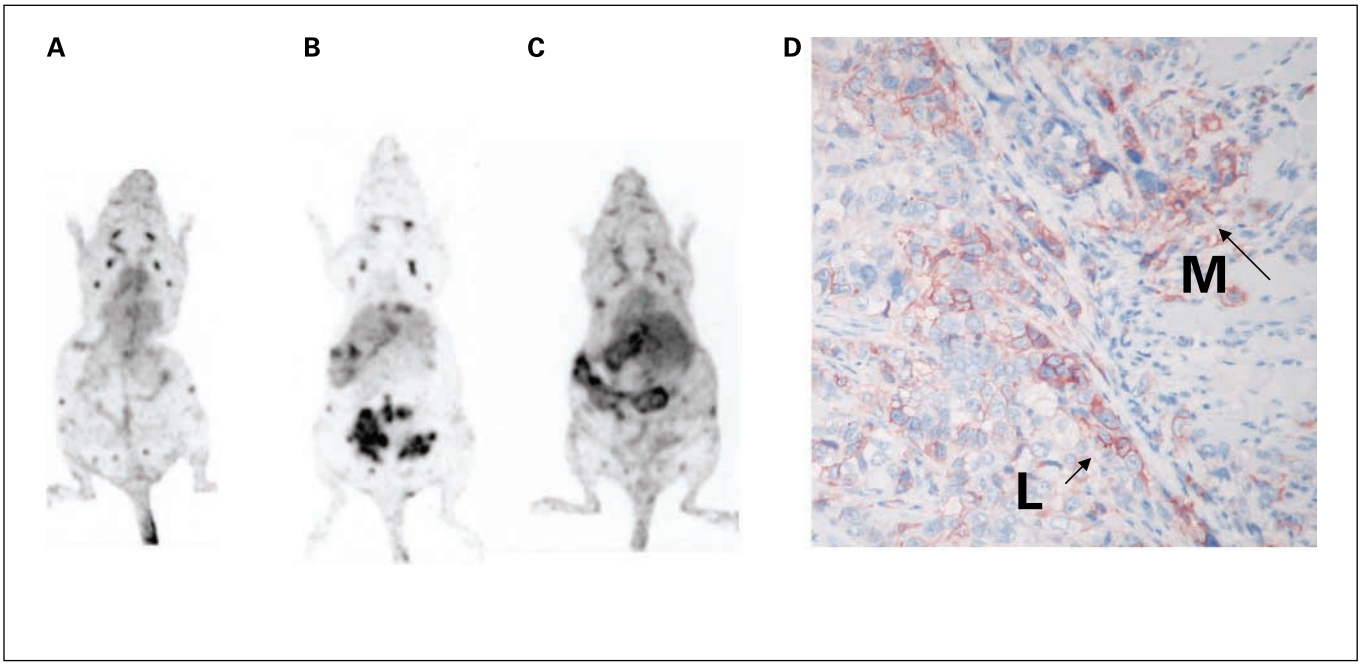

Fig. 3. PET imaging of three mice with ^{64}Cu-labeled anti-L1 mAb chCE7 (*A* and *B*) and anti-L1 mAb 11A (*C*). Paraffin section through a SKOV3ip tumor stained for L1 expression (*D*). *A,* tumor-free mouse; *B* and *C,* animals with abdominal SKOV3ip metastases. PET imaging was 21 to 23 h postinjection of ^{64}Cu-mAbs. Maximal intensity projection (presenting three-dimensional data in two dimensions) of the whole mouse body. *D,* immunohistochemical staining for L1 using mAb L1-14.10. Heterogeneous expression with L1-positive cells in the leading edge of the tumor (*L*) and in tumor cells invading the muscle tissue (*M*); L1-negative cells in the tumor mass.

quantitatively removed and measured. Tumor masses of such moribund animals ranged between 0.9 and 2.2 g.

Figure 4 shows Kaplan-Meier survival curves. In the first experiment (A), treatment of mice with biweekly doses of unlabeled mAb L1-11A was assessed and was found to prolong survival from 42 days (untreated controls) to 65 days, the difference not being statistically different (P = 0.1767). In a second experiment (B) a single dose of 10.5 MBq ^{67}Cu-CPTA–labeled chCE7agl prolonged the median survival from 31 to 51 days and showed significantly longer survival than controls (P = 0.0335). In contrast, the ^{67}Cu-CPTA-labeled control antibody (Lym1) showed a median survival of 34 days compared with controls (31 days) and the difference in survival was not statistically significant (P = 0.6572). In the third experiment (C), 14×10^6 SKOV3ip cells were inoculated in contrast to the other experiments in which 7×10^6 cells were inoculated. In this experiment, untreated animals with a low, suboptimal (5 MBq) dose of ^{67}Cu-chCE7agl and the combination of ^{67}Cu-chCE7agl with biweekly treatment with mAb L1-11A were evaluated. When data was analyzed by Kaplan-Meier plots, controls showed a median survival of 29 days. Animals given a single 5 MBq dose of control mAb ^{67}Cu-Lym-1 showed median survival of 33 days, the same as animals treated with a single 5 MBq dose of ^{67}Cu-chCE7agl. The combination of ^{67}Cu-chCE7agl with biweekly doses of 10 mg/kg of mAb L1-11A extended median survival to 61 days. Mice treated with a single dose of 5 MBq ^{67}Cu-labeled irrelevant mAb Lym1 showed no significant difference compared with mice with no treatment at all (P = 0.0751). A single dose of 5 MBq ^{67}Cu-chCE7agl also showed no statistically significant difference in survival compared with the controls (P = 0.0744). Mice that received ^{67}Cu-labeled chCE7agl in combination with unlabeled mAb L1-11A showed a statistically significant longer survival than the mice that received no treatment at all (P = 0.0063), and the difference between the combination therapy and therapy with a single low dose of ^{67}Cu-chCE7agl was also significant (P = 0.046).

Taken together, the results show that high-dose radioimmunotherapy is more effective than single low-dose radioimmunotherapy and multiple dosing with unlabeled mAb L1-11A. A combination of low-dose radioimmunotherapy with unlabeled mAb L1-11A prolonged survival significantly compared with the single treatments.

Discussion

MAbs can exert antitumor activity by stimulating the cellular immune response and recruiting T cells to the tumor site or by directly inhibiting the growth of tumor cells via induction of apoptosis and/or inhibition of growth signaling. In addition, mAbs mediate target-specific cell killing when they are coupled with cytotoxic drugs or radionuclides. When used for therapeutic strategies, all of these antibody-induced antitumor effects have been observed, but none have been proved entirely satisfactory in eradicating tumors. Loss of the target antigen by mutation and outgrowth of antigen-negative tumor cells is not the only reason for suboptimal efficacy. Mutations in the target protein and in different signaling pathways also contribute to the reduced efficacy of antibody-mediated growth inhibition (32, 33). For this reason, antibodies loaded with cytotoxic radionuclides (radioimmunotherapy) could increase the efficacy of antibody therapies. For instance, in patients with non–Hodgkin's lymphoma, ^{90}Y-ibritumomab (Zevalin) produced significantly higher overall and complete response rates than did the corresponding unlabeled growth-inhibitory rituximab (Rituxan; refs. 34, 35). In contrast, the failure of i.p. therapy of

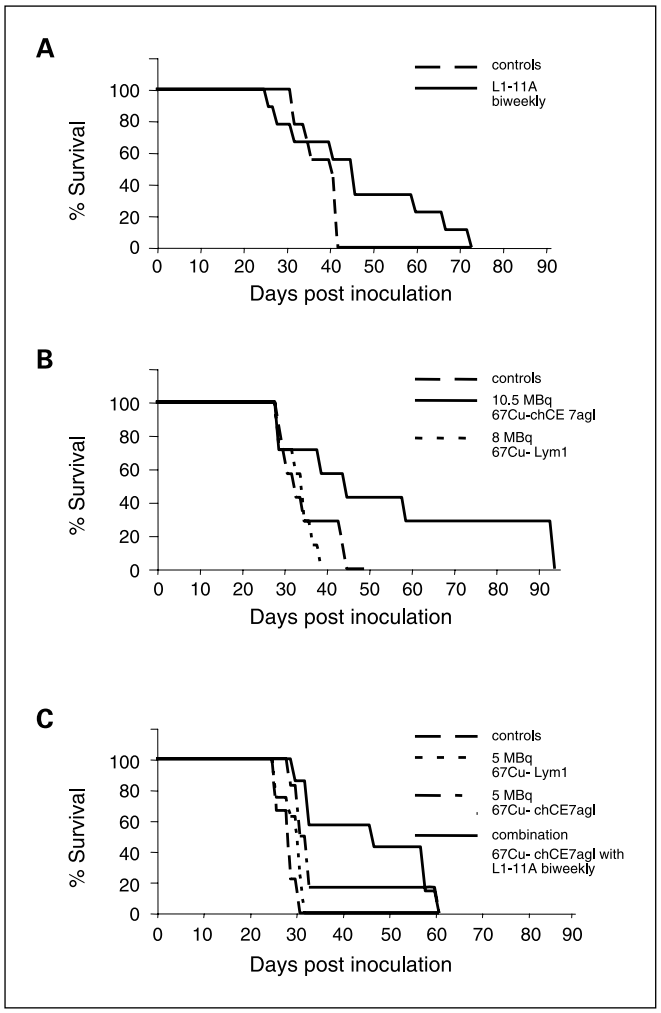

Fig. 4. ^{67}Cu-radioimmunotherapy and combination therapy with antibody L1-11A of SKOV3ip human ovarian cancer metastases in nude mice. *A,* Kaplan-Meier plots of the survival of groups of animals (n = 8-9) inoculated i.p. with 7×10^6 SKOV3ip cells. Two days postinoculation, no treatment (*controls*), treatment with 10 mg/kg of unlabeled anti-L1 mAb L1-11A biweekly i.p. The trend to increased survival after treatment with L1-11A was not significant ($P > 0.005$). *B,* Kaplan-Meier plots of the survival of groups of animals (n = 7-8) inoculated i.p. with 7×10^6 SKOV3ip cells. Two days postinoculation, no treatment (*controls*), treatment with a single i.v. dose of 8 MBq of ^{67}Cu-Lym1, a single i.v. dose of 10 MBq of ^{67}Cu-chCE7agl. Mice treated with ^{67}Cu-chCE7agl showed significantly increased survival ($P = 0.033$) compared with controls. *C,* Kaplan-Meier plots of the survival of groups of animals (n = 6-9) inoculated i.p. with 14×10^6 SKOV3ip cells. Two days postinoculation no treatment (*controls*), treatment with a single i.v. dose of 5 MBq of ^{67}Cu-Lym1, a single i.v. dose of 5 MBq of ^{67}Cu-chCE7agl, and the combination of a single i.v. dose of 5 MBq of ^{67}Cu-chCE7agl plus biweekly i.p. doses of mAb L1-11A. Mice which were treated with a combination of mAb L1-11A and 67Cu-chCE7agl showed significantly better survival ($P = 0.006$).

epithelial ovarian cancer with ^{90}Y-muHMFG1 antibody, which was reported recently in a large phase III study (4), indicates the importance of improved tumor targeting for this disease. Although the bulk of ovarian cancer resides in the i.p. space, sometimes, distant metastases can be detected in lymph nodes and bone marrow and i.v. application may be an advantage. For i.v. application, pharmacokinetics of the antibodies should exhibit a half-life in the blood sufficiently long to achieve high accumulation of radioactivity at the tumor site. At the same time, the levels in normal tissues such as kidney and liver should be minimized. The radiocopper-labeled chCE7agl construct we selected for therapy experiments combines these properties and shows consequently excellent tumor targeting in the SKOV3ip metastases model. Efficient internalization of the radiocopper-labeled chCE7agl mutant in target tumor cells contributes to the prolonged tumor residence.

We also evaluated mutations of residues in the Fc region which regulate binding to the FcRn receptor and had been found to reduce the half-life of the radioiodinated immunoglobulins in the blood (22, 36). A series of antibody fragments with β half-lives in the blood ranging from 83 to 8 h had been generated by this approach (22). Following this concept, we found that a H310A mutation reduced the β half-life in the blood of radioiodinated chCE7 (150 kDa) >10-fold, and for the ^{67}Cu-labeled immunoconjugate, an ~7-fold reduced half-life was observed. An aglycosylated chCE7 mutant N297Q (chCE7agl), showed a more modest ~50% reduction in half-life. The biodistributions of the two mutant mAbs were compared in ^{67}Cu-labeled form and the H310A mutant showed about four times lower tumor uptake and about two times higher levels of radioactivity in the liver. Consequently, the N297Q (agl) mutant was chosen for therapy experiments.

To test therapeutic efficacy, the SKOV3ip orthotopic metastases model was chosen. The fact that therapy had already started 2 days postinoculation of cells indicates that it is not a model for treating widespread ovarian cancer, but rather, that it may represent the situation of micrometastatic disease. In mouse models of i.p. metastases, therapeutic effects in terms of prolonged survival were observed with radioimmunotherapy using radiometal-labeled antibodies, including a domain-deleted mAb (37–39). No complete cures were achieved in these models of aggressive metastatic disease.

We tested single i.v. doses of radiocopper-labeled anti-L1 mAb chCE7agl. The i.v. route for injection of the radiocopper conjugate as opposed to the frequently propagated i.p. administration was chosen because it may be relevant for both imaging and treatment of distant metastases. PET imaging with ^{64}Cu-labeled antibodies would be very useful to select patients and to provide dosimetry and may be of value in following the course of the disease and efficacy of treatments. The shortened half-life in the blood of the ^{67}Cu-chCE7agl compared with the parent mAb is an improvement for both imaging as well as for therapy. We found that a low 4 MBq dose of ^{67}Cu-chCE7agl led to an already significant reduction of tumor burden similar to the effect achieved with a 10.5 MBq dose (Table 3). However, when survival was analyzed, this low dose did not prolong survival significantly, in contrast to the 10 MBq dose which led to significantly increased survival (Fig. 4). In addition, in these survival experiments, we asked how the efficiency of radioimmunotherapy with ^{67}Cu-labeled anti-L1 mAb chCE7agl compares with growth inhibition using anti-L1 mAb L1-11A. Many possible combinations could be envisaged. For a first evaluation of the feasibility of this approach, we chose a survival experiment combining biweekly treatment with unlabeled mAb L1-11A with low-dose radioimmunotherapy with 5 MBq of ^{67}Cu-chCE7agl. We found that the single treatments did not significantly prolong the survival of control animals. The heterogeneous expression of L1 observed in the SKOV3ip tumor masses (Fig. 3D) could explain why therapy with unlabeled mAb L-11A showed no significant increase in survival, whereas high-dose radioimmunotherapy with 10.5 MBq of ^{67}Cu-chCE7agl led to a significantly longer survival, the

effect of radiation being effective over several cell diameters. The specificity of radioimmunotherapy is shown in the experiment with the ^{67}Cu-labeled Lym-1 antibody used as a nonbinding IgG_1 control antibody which showed no significant effects on survival. To date, only one study on the efficacy of ^{67}Cu-radioimmunotherapy in nude mice with s.c. xenografts of human Burkitt lymphoma has been done (40), and the maximal tolerated dose was ~20 MBq of ^{67}Cu-labeled mAb Lym-1 dosing, starting at 12 MBq. Increasing doses to 18.5 MBq showed no dose-dependent effect in this solid tumor model, and the authors discuss the potential adding synergistic agents. Our results in the SKOV3ip metastases model show significant tumor reduction and increased survival with a single 10.5 MBq dose of ^{67}Cu-chCE7agl. A combination of unlabeled anti-L1 mAb L1-11A with a single low-dose ^{67}Cu-radioimmunotherapy prolonged survival significantly, the data indicating the advantages of combining anti–L1-directed growth inhibition with radioimmunotherapy for the therapy of ovarian cancer metastases.

Acknowledgments

We thank Prof. B. Seifert (Department of Biostatistics, University of Zurich) for helping with the statistical analysis of the therapy studies. Support from Drs. Achim Krüger and Matthias Arlt (Technical University of Munich) with the SKOV3ip model in the initial phase of the study is highly appreciated.

References

1. Nicodemus CF, Berek JS. Monoclonal antibody therapy of ovarian cancer. Expert Rev Anticancer Ther 2005;5:87–96.
2. Tuma RS. Success of bevacizumab trials raises questions for future studies. J Natl Cancer Inst 2005;97:950–1.
3. Monk BJ, Choi DC, Pugmire G, et al. Activity of bevacizumab (rhuMAB VEGF) in advanced refractory epithelial ovarian cancer. Gynecol Oncol 2005;96:902–5.
4. Verheijen RH, Masuger LF, Benigno BB, et al. Phase III trial of intraperitoneal therapy with yttrium-90-labeled HMFG1 murine monoclonal antibody in patients with epithelial ovarian cancer after a surgically defined complete remission. J Clin Oncol 2006;24:571–8.
5. Mahe MA, Fumoleau P, Fabbro M, et al. A phase II study of intraperitoneal radioimmunotherapy with iodine-131-labeled monoclonal antibody OC-125 in patients with residual ovarian carcinoma. Clin Cancer Res 1999;5:3249–53s.
6. Arlt MJ, Novak-Hofer I, Gast D, et al. Efficient inhibition of intra-peritoneal tumor growth and dissemination of human ovarian carcinoma cells in nude mice by anti-L1-cell adhesion molecule monoclonal antibody treatment. Cancer Res 2006;66:936–43.
7. Kamiguchi H, Long KE, Pendergast M, et al. The neural cell adhesion molecule L1 interacts with the AP-2 adaptor and is endocytosed via the clathrin-mediated pathways. J Neurosci 1998;18:5311–21.
8. Hulley P, Schachner M, Lubbert H. L1 neural cell adhesion molecule is a survival factor for fetal dopaminergic neurons. J Neurosci Res 1998;53:129–34.
9. Runker AE, Bartsch U, Nave KA, et al. The C264Y missense mutation in the extracellular domain of L1 impairs protein trafficking *in vitro* and *in vivo*. J Neurosci 2003;23:277–86.
10. Meli ML, Carrel F, Waibel R, et al. Anti-neuroblastoma antibody chCE7 binds to an isoform of L1-CAM present in renal carcinoma cells. Int J Cancer 1999;83:401–8.
11. Heiz M, Grunberg J, Schubiger PA, et al. Hepatocyte growth factor-induced ectodomain shedding of cell adhesion molecule L1: role of the L1 cytoplasmic domain. J Biol Chem 2004;279:31149–56.
12. Fogel M, Mechtersheimer S, Huszar M, et al. L1 adhesion molecule (CD171) in development and progression of human malignant melanoma. Cancer Lett 2003;189:237–47.
13. Fogel M, Gutwein P, Mechtersheimer S, et al. L1 expression as a predictor of progression and survival in patients with uterine and ovarian carcinomas. Lancet 2003;362:869–75.
14. Gavert N, Conacci-Sorrell M, Gast D, et al. L1, a novel target of β-catenin signaling, transforms cells and is expressed at the invasive front of colon cancers. J Cell Biol 2005;168:633–42.
15. Mechtersheimer S, Gutwein P, Agmon-Levin N, et al. Ectodomain shedding of L1 adhesion molecule promotes cell migration by autocrine binding to integrins. J Cell Biol 2001;155:661–73.
16. Silletti S, Yebra M, Perez B, et al. Extracellular signal-regulated kinase (ERK)-dependent gene expression contributes to L1 cell adhesion molecule-dependent motility and invasion. J Biol Chem 2004;279:28880–8.
17. Primiano T, Baig M, Maliyekkel A, et al. Identification of potential anticancer drug targets through the selection of growth-inhibitory genetic suppressor elements. Cancer Cell 2003;4:41–53.
18. Novak-Hofer I, Amstutz HP, Haldemann A, et al. Radioimmunolocalization of neuroblastoma xenografts with chimeric antibody chCE7. J Nucl Med 1992;33:231–6.
19. Novak-Hofer I, Amstutz HP, Macke HR, et al. Cellular processing of copper-67-labeled monoclonal antibody chCE7 by human neuroblastoma cells. Cancer Res 1995;55:46–50.
20. Novak-Hofer I, Amstutz HP, Morgenthaler JJ, et al. Internalization and degradation of monoclonal antibody chCE7 by human neuroblastoma cells. Int J Cancer 1994;57:427–32.
21. Hoefnagel CA, Rutgers M, Buitenhuis CK, et al. A comparison of targeting of neuroblastoma with mIBG and anti L1-CAM antibody mAb chCE7: therapeutic efficacy in a neuroblastoma xenograft model and imaging of neuroblastoma patients. Eur J Nucl Med 2001;28:359–68.
22. Kenanova V, Olafsen T, Crow DM, et al. Tailoring the pharmacokinetics and positron emission tomography imaging properties of anti-carcinoembryonic antigen single-chain Fv-Fc antibody fragments. Cancer Res 2005;65:622–31.
23. Medesan C, Matesoi D, Radu C, et al. Delineation of the amino acid residues involved in transcytosis and catabolism of mouse IgG1. J Immunol 1997;158:2211–7.
24. Sambrook J, Russel D. Molecular cloning: a laboratory manual. 3rd ed. CSH Laboratory Press, Cold Spring Harbor (NY); 2001.
25. Grunberg J, Knogler K, Waibel R, et al. High-yield production of recombinant antibody fragments in HEK-293 cells using sodium butyrate. Biotechniques 2003;34:968–72.
26. Zimmermann K, Grunberg J, Honer M, et al. Targeting of renal carcinoma with 67/64Cu-labeled anti-L1-CAM antibody chCE7: selection of copper ligands and PET imaging. Nucl Med Biol 2003;30:417–27.
27. Schwarzbach R, Zimmermann K, Blauenstein P, et al. Development of a simple and selective separation of 67Cu from irradiated zinc for use in antibody labelling: a comparison of methods. Appl Radiat Isot 1995;46:329–36.
28. Lindmo T, Boven E, Cuttitta F, et al. Determination of the immunoreactive fraction of radiolabeled monoclonal antibodies by linear extrapolation to binding at infinite antigen excess. J Immunol Methods 1984;72:77–89.
29. Zimmermann K, Gianollini S, Schubiger PA, et al. A triglycine linker improves tumor uptake and biodistributions of 67-Cu-labeled anti-neuroblastoma MAb chCE7 F(ab')2 fragments. Nucl Med Biol 1999;26:943–50.
30. Mikolajczyk K, Szabatin M, Rudnicki P, et al. A JAVA environment for medical image data analysis: initial application for brain PET quantitation. Med Inform (Lond) 1998;23:207–14.
31. Huszar M, Moldenhauer G, Gschwend V, et al. Expression profile analysis in multiple human tumors identifies L1 (CD171) as a molecular marker for differential diagnosis and targeted therapy. Hum Pathol 2006;37:1000–8.
32. Bates SE, Fojo T. Epidermal growth factor receptor inhibitors: a moving target? Clin Cancer Res 2005;11:7203–5.
33. Grunberg J, Novak-Hofer I, Honer M, et al. *In vivo* evaluation of 177Lu- and 67/64Cu-labeled recombinant fragments of antibody chCE7 for radioimmunotherapy and PET imaging of L1-CAM-positive tumors. Clin Cancer Res 2005;11:5112–20.
34. Witzig TE, Gordon LI, Cabanillas F, et al. Randomized controlled trial of yttrium-90-labeled ibritumomab tiuxetan radioimmunotherapy versus rituximab immunotherapy for patients with relapsed or refractory low-grade, follicular, or transformed B-cell non-Hodgkin's lymphoma. J Clin Oncol 2002;20:2453–63.
35. DeNardo GL. Treatment of non-Hodgkin's lymphoma (NHL) with radiolabeled antibodies (mAbs). Semin Nucl Med 2005;35:202–11.
36. Kenanova V, Wu AM. Tailoring antibodies for radionuclide delivery. Expert Opin Drug Deliv 2006;3:53–70.
37. Janssen ML, Pels W, Massuger LF, et al. Intraperitoneal radioimmunotherapy in an ovarian carcinoma mouse model: effect of the radionuclide. Int J Gynecol Cancer 2003;13:607–13.
38. Milenic DE, Garmestani K, Brady ED, et al. Targeting of HER2 antigen for the treatment of disseminated peritoneal disease. Clin Cancer Res 2004;10:7834–41.
39. Rogers BE, Roberson PL, Shen S, et al. Intraperitoneal radioimmunotherapy with a humanized anti-TAG-72 (CC49) antibody with a deleted CH2 region. Cancer Biother Radiopharm 2005;20:502–13.
40. DeNardo GL, Kukis DL, Shen S, et al. Efficacy and toxicity of 67-2IT-BAT-Lym-1 radioimmunoconjugate in mice implanted with human Burkitt's lymphoma (Raji). Clin Cancer Res 1997;3:71–9.

Clinical Cancer Research

Copper-67 Radioimmunotherapy and Growth Inhibition by Anti–L1-Cell Adhesion Molecule Monoclonal Antibodies in a Therapy Model of Ovarian Cancer Metastasis

Karin Knogler, Jürgen Grünberg, Kurt Zimmermann, et al.

Clin Cancer Res 2007;13:603-611.